

Nonconventional tight-binding method for the calculation of the total energy and spectroscopic energies of atomic clusters: Transferable parameters for silicon

Z. M. Khakimov,* P. L. Tereshchuk, N. T. Sulaymanov, and F. T. Umarova
Institute of Nuclear Physics of Uzbekistan Academy of Sciences, Tashkent 702132, Uzbekistan

M. T. Swihart

Department of Chemical and Biological Engineering, University at Buffalo, State University of New York, Buffalo, New York 14260-4200, USA

(Received 27 June 2005; published 27 September 2005)

The principal differences between conventional tight-binding methods and a nonconventional tight-binding method proposed earlier by one of the authors [Z. M. Khakimov, *Comput. Mater. Sci.* **3**, 95 (1994)] are highlighted here. The latter has been optimized for simulation of the structure, cohesive energies, ionization potentials, and electronic affinities of silicon clusters. A single tight-binding approximation has been used to predict all of the above properties with accuracy comparable to state-of-the-art *ab initio* methods. This demonstrates the potential of tight-binding methods as a quantitative, predictive tool, provided they are based on an accurate total energy functional and exploit properly the individual properties of chemical elements, accounting for both intra- and interatomic charge redistributions.

DOI: [10.1103/PhysRevB.72.115335](https://doi.org/10.1103/PhysRevB.72.115335)

PACS number(s): 73.22.-f, 61.46.+w, 71.15.Nc

I. INTRODUCTION

The tight-binding (TB) approach introduced by Slater and Koster¹ and developed by Harrison² for the simplified estimation of a variety of properties of solids has become a popular and convenient tool for total energy calculations and molecular dynamics simulations. It offers a reasonable compromise between classical interaction potentials and *ab initio* electronic structure calculation methods, being rather close in efficiency to the former due to strong simplifications in the electronic structure calculations. In the last two decades much attention has been paid to development of different TB models, particularly for silicon,^{3–23} applying them for simulations of the structure and stability of both defects in bulk material and atomic clusters. In particular, density functional-based TB (DFTB) (Ref. 15) was very helpful in determining possible low-energy isomers of silicon clusters,²³ providing initial guess geometries for computationally expensive first-principles calculations. One can also find successful applications of this TB model in chemistry and biology.²⁴ However, this model inherits disadvantages of both the local density approximation (LDA) and conventional TB methods that lead to overestimation of cohesive energies and bond distances for silicon clusters, respectively. Because of the ever-increasing importance of TB models for complex systems and unknown structures, particularly for the rich variety of possible nanostructures where the environment of the atoms is intermediate between the molecular and bulk environments, the development of highly accurate and transferable TB models of other types is of great importance.

Conventional TB total energy calculation models are based on a total energy functional of the following form:^{3,9,22}

$$E_{tot} = \tilde{E}_{rep} + E_{band} - \Delta\tilde{E}. \quad (1)$$

Here, E_{band} is the so-called band structure energy, the sum of energies of occupied electronic states, which can also be written as

$$E_{band} = \sum_{\mu,\nu} \sum_{i,j} P_{\mu i, \nu j} H_{\mu i, \nu j}, \quad (2)$$

where $H_{\mu i, \nu j}$ and $P_{\mu i, \nu j}$ are Hamiltonian and bond-order matrix elements, μ and ν denote nuclei, and i and j denote atomic orbitals (AO). This term includes electron-electron interaction energy (E_{ee}) twice, so this extra inclusion must be removed. As TB does not treat E_{ee} explicitly (it is parametrized implicitly together with $H_{\mu i, \nu j}$), Chadi³ proposed avoiding this difficulty by introducing a single repulsive energy term of the form

$$\tilde{E}_{rep} = E_{nn} - E_{ee}^{inter}, \quad (3)$$

where E_{nn} and E_{ee}^{inter} are nuclear-nuclear and interatomic electron-electron interaction energies, respectively. This term is then approximated by a sum of simple analytical functions of interatomic distances. Because \tilde{E}_{rep} involves complex nonpairwise electron-electron interaction energies, it cannot be represented reliably by pairwise functions. On the other hand, the introduction of complex embedding functionals that explicitly or implicitly depend on the number of chemical bonds (or neighboring atoms) did not lead to significant improvement of these results, but did introduce new difficulties associated with ambiguity in defining the number of chemical bonds. In fact, none of the functional forms for \tilde{E}_{rep} and $H_{\mu i, \nu j}$ proposed in the literature has been found^{19,22} to be clearly superior to others.

Apart from the above, conventional TB models strongly underestimate the role of the last term in Eq. (1). $\Delta\tilde{E}$ is either the *intraatomic* part (E_{ee}^{intra}) of E_{ee} or the sum of the energies of occupied AO⁹ of isolated atoms, provided that total energy is measured relative to that of isolated atoms and charge redistribution among both AO of the same atom and different atoms is neglected. However, even in this approximation de-

velopers of TB have often used $\Delta\tilde{E}$ arbitrarily, in particular, as an *ad hoc* total energy corrector term^{8,12} or sum of AO energies with values that differ significantly not only from exact results for the silicon atom, but also in different TB parametrizations;^{6,11,19} in fact these values are not representative of Si.

Development of conventional TB total energy calculation models has been mostly driven by the desire to have the simplest electronic structure-based computational approach possible, while accuracy and transferability problems have been addressed by increasing the complexity of functional forms for terms in Eq. (1), as well as by increasing the number of fitting parameters and reference systems. For this approach to succeed, the modifications of the TB functionals must incorporate more of the chemistry and physics of the system in question. Particular attention must be paid to self-consistent charge calculations that naturally account for different atomic environments that occur in realistic systems, including nanoscale systems. The tight-binding model¹⁴ previously developed by one of us is an attempt to do this. It is based on a different total energy functional and relies on individual properties of chemical elements for determining its fundamental parameters. This model, which we will call the nonconventional tight-binding (NTB) model, even with a simple parametrization, was able to treat correctly²⁵ such properties of defects in silicon as the negative- U property of Si vacancies and the electron-enhanced low energy migration of Si self-interstitials. It also predicted the electrical levels of a number of impurities without using Koopmans' theorem. These are not applications where conventional TB can typically succeed. In this paper we present the development of NTB for calculating the geometry, cohesive energy, ionization potentials (IP), and electronic affinities (EA) of atomic clusters and apply it to simultaneously predict all of these properties accurately for small and medium-size silicon clusters.

NTB¹⁴ is based on the following total energy functional:

$$E_{tot} = E_{rep} + E_{bond} + \Delta E. \quad (4)$$

Here, E_{bond} includes terms only with $\mu > \nu$ from Eq. (2), so that it is a *pure* bond energy, containing the interatomic part of the electronic energy only once (in the literature one can find improper definitions of bond energy as twice this; see for instance, Ref. 16). ΔE is the sum of changes in total energy of individual atoms with respect to isolated atoms, which can be parametrized by a modified Slater-Zerner formula,¹⁴ without explicitly addressing E_{ee}^{intra} , and by using rich and accurate spectroscopic data on atoms and ions. The repulsive term has quite simple physical content,

$$E_{rep} = E_{nn} - E_{ee}^{inter} + E_{bond} \cong E_{nn} + E_{ne}^{inter}, \quad (5)$$

as it does not include more the complex E_{ee}^{inter} term; this term is canceled out in the difference $E_{bond} - E_{ee}^{inter}$,¹⁴ leaving the much simpler E_{ne}^{inter} term, which is one-half of the attraction energy of electrons localized around one nucleus to other nuclei. (To contrast the difference between the two repulsive terms, Eqs. (3) and (5), the two-center electron kinetic en-

ergy term is not shown in Eq. (5); the approximate sign reflects this.)

Note that Eq. (1) can also be written in the form

$$E_{tot} = \tilde{E}_{rep} + 2E_{bond} + \Delta E, \quad (1')$$

which is used in the bond-order form of TB,¹⁶ but again with less attention paid to the last term for efficiency reasons, imposing a local charge neutrality requirement. Comparing Eqs. (1') and (4), one finds that E_{rep} includes shorter-range interactions than \tilde{E}_{rep} . $E_{rep} \approx \tilde{E}_{rep}/2$ near typical bond distances and $E_{rep} \ll \tilde{E}_{rep}$ at large distances (this is also a result of the functional form of E_{rep} ; see the next section), provided that E_{bond} and ΔE have the same values in both equations. Because of this and its simple physical content, E_{rep} can be more reliably represented by a sum of pairwise functions of interatomic distances than \tilde{E}_{rep} , which is important for both efficiency and accuracy of calculations. This also immediately suggests that the long-range character of \tilde{E}_{rep} is perhaps the main reason for systematic overestimation of bond distances in silicon clusters by conventional TB. Thus, NTB should be more suitable for parametrization and minimization of errors of semiempirical total energy calculations than conventional TB.

The remainder of this paper is organized as follows. The second section describes NTB (Ref. 14) with modifications made in this work and its use in molecular dynamics simulations, as well as other computational details. The third section presents a NTB parametrization for silicon using experimental and *ab initio* data for small silicon clusters consisting of up to seven atoms. The fourth section contains results of our calculations for silicon clusters Si_n with $7 < n \leq 20$. Comparison of our results with those of accurate *ab initio* and other TB calculations are made in both the third and fourth sections. The last section summarizes the main conclusions of the work.

II. NONCONVENTIONAL TIGHT-BINDING METHOD

The total energy functional (4) of NTB¹⁴ is rewritten in more detail as Eq. (6),

$$E_{tot} = \sum_{\mu} \sum_{\nu > \mu} \frac{Z_{\mu}^{scr} Z_{\nu}^{scr}}{R_{\mu\nu}} + \sum_{\mu} \sum_{\nu > \mu} \frac{Q_{\mu} Q_{\nu}}{R_{\mu\nu}} + \sum_{\mu} \sum_{\nu > \mu} \sum_i \sum_j P_{\mu i, \nu j} H_{\mu i, \nu j} + \sum_{\mu} (E_{\mu} - E_{\mu}^0), \quad (6)$$

where $R_{\mu\nu}$ is the internuclear distance,

$$Z_{\mu}^{scr} = Z_{\mu}^{scr}(R_{\mu\nu}, \{N_{\mu i}^0\}) = Z_{\mu} - \sum_i N_{\mu i}^0 [1 - a_{\mu i} \exp(-\alpha_{\mu i} R_{\mu\nu} / R_{\mu i}^0)], \quad (7)$$

$$Q_{\mu} = Z_{\mu}^{scr}(R_{\mu\nu}, \{N_{\mu i}^0\}) - Z_{\mu}^{scr}(R_{\mu\nu}, \{N_{\mu i}\}), \quad (8)$$

are screened nuclear and nonpoint ionic charges, respectively; Z_{μ} is the charge of the μ th nucleus (or nucleus plus core electrons); $R_{\mu i}^0 = n_{\mu i} / \xi_{\mu i}^0$ is the most probable distance

between the i th electron and the corresponding μ th nucleus, $n_{\mu i}$ and $\xi_{\mu i}^0$ are the principal quantum number and Slater exponent of i th AO centered at the μ th nucleus; E_{μ}^0 and E_{μ} are the total energies of individual atoms in noninteracting and interacting systems characterized by sets of occupancy numbers $\{N_{\mu i}^0 \equiv P_{\mu i, \mu i}^0\}$ and $\{N_{\mu i} \equiv P_{\mu i, \mu i}\}$ and energies $\{E_{\mu i}^0\}$ and $\{E_{\mu i}\}$ of valence AOs, respectively. Note the repulsive term is defined¹⁴ as repulsion of screened nuclear charges of neutral atoms in ground states, while accounting for effect of intraatomic and interatomic charge redistributions is delegated to the ion-ion interaction term for the sake of convenience. Therefore, the second term in Eq. (6) may be nonzero even for a neutral atom, say, due to hybridization of valence AOs; for this reason this term can be called a “generalized” ion-ion interaction energy term. In formulas, hereafter, α , β , γ , a , b , d , e are fitting parameters, distances are in bohr, energies are in hartrees, and charges are in the electron charge unit.

AOs are presumed to be orthogonal and a matrix equation of the form

$$\sum_{vj} (H_{\mu i, vj} - \varepsilon \delta_{\mu i, vj}) C_{vj} = 0 \quad (9)$$

is solved self-consistently to obtain electronic spectra $\{\varepsilon_k\}$ and AO expansion coefficients $\{C_{vj}(k)\}$ of molecular orbitals (MO) of the system. Self-consistent calculations are performed by iterative recalculation of diagonal elements of the Hamiltonian matrix elements using the dependence of the bond-order matrix

$$P_{\mu i, vj} = \sum_k N_k C_{\mu i}(k) C_{vj}(k) \quad (10)$$

and AO occupancy numbers $N_{\mu i} \equiv P_{\mu i, \mu i}$ on the AO expansion coefficients $C_{vj}(k)$. Here k denotes a MO and N_k denotes the occupancy number of the k th MO. In conventional TB, the N_k are all equal to 2 (except the highest MO of a system with an odd number of electrons). However, NTB is aimed at treating charged and excited states etc., where several highest occupied MOs may have occupations less than 2.

Diagonal and off-diagonal Hamiltonian matrix elements of NTB are

$$H_{\mu i, \mu j} = \left(E_{\mu i} - \sum_{\nu \neq \mu} Q_{\nu} / R_{\mu \nu} \right) \delta_{ij}, \quad (11)$$

and

$$H_{\mu i, \nu j} = \pm \frac{1}{2} h_{\mu i} h_{\nu j} A_{ij}(\vec{R}_{\mu \nu}), \quad \nu \neq \mu, \quad (12)$$

respectively, where

$$h_{\mu i} = b_{\mu i} \xi_{\mu i}^0 \exp(-\beta_{\mu i} R_{\mu i} / 2 \bar{R}_{\mu i}^0) F_{\mu i}, \quad (13)$$

$$F_{\mu i} = \{1 + \exp[-\gamma_{\mu i}(R_{\mu \nu} - d_{\mu i})]\}^{-1}, \quad (14)$$

$\bar{R}_{\mu i}^0 = (n_{\mu i} + 1/2) / \xi_{\mu i}^0$ is the mean distance between electron and corresponding nucleus, and $A_{ij}(\vec{R}_{\mu \nu})$ are angular functions tabulated by Slater and Koster.^{1,2} In Eq. (12) the negative sign is taken for ss and $pp-\pi$ matrix elements, while the positive sign is taken for sp and $pp-\sigma$ matrix elements. In the

general case, matrix elements (12) between p -AOs result from mixing of $pp-\pi$ and $pp-\sigma$ matrix elements, which preserves invariance of the results with respect to rotation of the coordinate system.

$E_{\mu i}$ and E_{μ} are defined by formulas¹⁴

$$E_{\mu i} = E_{\mu i}(\{N_{\mu j}\}) = -\frac{1}{2} \left[Z_{\mu i}^{\text{eff}} + \sum_j q_{\mu j} S_{ij} + \Delta_{\mu i}^{\text{corr}} \right]^2 / [n_{\mu i} n_{\mu i}^{\text{eff}}(q_{\mu})], \quad (15)$$

$$E_{\mu} = \frac{1}{2} \sum_i N_{\mu i} [E_{\mu i}(\{N_{\mu j}\}) + E_{\mu i}(1)], \quad (16)$$

where $E_{\mu i}(1)$ represents the energy of a valence s - or p -AO containing one electron, with other p - or s -AO empty,

$$Z_{\mu i}^{\text{eff}} = \xi_{\mu i}^0 n_{\mu i}^{\text{eff}}(0), \quad n_{\mu i}^{\text{eff}}(0) = -2E_{\mu i}^0 / (\xi_{\mu i}^0)^2 n_{\mu i}, \quad (17)$$

$$S_{ij} = 1 - \exp(-\bar{R}_{\mu i}^0 / R_{\mu j}^0), \quad (18)$$

$$n_{\mu i}^{\text{eff}}(q) = n_{\mu i}^{\text{eff}}(0) + [n_{\mu i} - n_{\mu i}^{\text{eff}}(0)] q_{\mu} / (Z_{\mu} - 1), \quad \mu > 1, \quad (19)$$

$$\Delta_{\mu s}^{\text{corr}} = \Delta e_1 q_{\mu s} + \Delta e_2 q_{\mu p} + \Delta e_3 (q_{\mu})^2, \quad (20a)$$

$$\Delta_{\mu p}^{\text{corr}} = \Delta e_4 q_{\mu s} + \Delta e_5 q_{\mu p} + \Delta e_6 (q_{\mu})^2, \quad (20b)$$

$$q_{\mu i} = N_{\mu i}^0 - N_{\mu i}, \quad q_{\mu} = \sum_i q_{\mu i}.$$

Note that this modification of the well-known Slater-Zerner formula consists of using a product of a quantum number and an effective quantum number in Eq. (15) instead of the square of the latter, and accepting linear dependence [Eq. (19)] of the latter on the charge state of the atoms, so that it will be equal to the corresponding quantum numbers of hydrogen for the case of an ion with one electron. As shown previously,¹⁴ the universal formula (18) for screening constants describes the energies of AOs of elements for their several charge states, as well as corresponding ionization potentials and electronic affinities reasonably well. Here we introduce fitting parameters through (20) for accurate reproduction of energies of several electronic transitions in atoms and ions. In fact, the first two fitting parameters in each formula (20) correct universal screening constants (18) and perhaps reflect also the accuracy of early *ab initio* data²⁶ on the energy of AO and Slater exponents, optimized by minimization of total energy of atoms in a minimal basis set. These data are given for almost all of the elements and are the basis for NTB.

The main differences between the present version of NTB and the original one¹⁴ are a new definition (8) for Q , and the addition of the Fermi-functionlike factor (14) for off-diagonal matrix elements, which provides extra flexibility for them and allows them to decay faster with increasing interatomic distance. The present version also incorporates more fitting parameters, taking advantage of a large database of

structural and energetic data on small silicon clusters to determine an optimal set of parameters. Thus, the number of fitting parameters increased from 3 in the original NTB¹⁴ to about 20 in the present version (see the next section).

Note, however, the special form of the NTB formulae, obtained as a generalization¹⁴ of the hydrogen molecule case and based on individual characteristics of chemical elements (energies and Slater exponents of AOs) does not initially require any fitting parameters. Except for the new parameters in Eq. (14), they are “normalized” such that they can be set equal to 1 [or 0 in Eq. (20)] and meaningful calculations can be performed even for heteronuclear systems. Of course, this feature of NTB, which is absent in other semiempirical methods, must be used with care and additional research must be done to improve it.

NTB is computationally more expensive than conventional TB because it incorporates self-consistent calculations. For converging these calculations, dynamical damping²⁷ and level shift²⁸ schemes are used. We implemented a very tight convergence test for clusters considered here, terminating every single point self-consistent calculation only when changes of atomic occupancy numbers in sequential iterations were less than 10^{-9} . Apart from this, forces are calculated numerically, because analytical derivatives cannot be obtained for the last term in (6) that only implicitly depends on the arrangement of atoms. However, numerical derivatives are beneficial to some extent when one implements the NTB within a molecular dynamics approach²⁹ using an alternative algorithm³⁰ for integration of equations of motion. In this third-order algorithm, which was shown to be more accurate than high-order predictor-corrector algorithms,^{30,31} positions, R , and velocities, v , of particles are advanced using the following equations:

$$R_{t+\delta t} = \left[R_t + v_t \delta t + \frac{1}{12}(7a_t - a_{t-\delta t}) \delta t^2 \right] \times \left[1 - \frac{1}{12} \frac{da_t}{dR_t} \delta t^2 \right]^{-1}, \quad (21)$$

$$v_{t+\delta t} = v_t + \frac{1}{12}[8a_t + 5a_{t+\delta t} - a_{t-\delta t}] \delta t, \quad (22)$$

where a_t is the acceleration of a particle with mass m at time t , and da_t/dR_t is its derivative with respect to the particle's position R . When forces (accelerations) are calculated numerically, their derivatives can be simultaneously obtained using the same two additional total energy values calculated at positions $R_t + \delta R$ and $R_t - \delta R$ (δR is a small shift),

$$a_t = - \frac{1}{m} \frac{E(R_t + \delta R) - E(R_t - \delta R)}{2\delta R}, \quad (23)$$

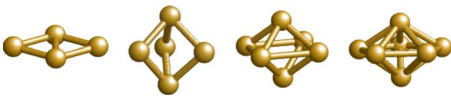


FIG. 1. (Color online) Equilibrium geometries of small silicon clusters (Ref. 38) fitted by NTB. Geometric parameters for these structures are given in Table III.

$$\frac{da_t}{dt} = - \frac{1}{m} \frac{E(R_t + \delta R) + E(R_t - \delta R) - 2E(R_t)}{\delta R^2}. \quad (24)$$

Note that in the NTB parametrization stage there is no need for molecular dynamics simulations because of the high symmetry of small compact clusters and the small number of geometric parameters to be optimized (see the next section). Therefore, a conjugate gradient technique is used for geometry optimizations needed in determining the NTB parameters.

III. PARAMETRIZATION OF NTB FOR SILICON USING DATABASE ON SMALL CLUSTERS

Charge and electronic state dependent energies of AOs, which define diagonal matrix elements, Eq. (11), and the last term of the NTB total energy functional, Eq. (6), were parametrized by fitting six parameters in (20) to the energies of following lowest electronic transitions between highest spin states of the silicon atom and ions:³² $s^2p^2 \rightarrow s^2p^3$ (-1.390 eV), $s^2p^2 \rightarrow s^2p^1$ (8.152 eV), $s^2p^1 \rightarrow s^2p^0$ (16.346 eV), $s^2p^2 \rightarrow s^1p^2$ (13.460 eV), $s^2p^2 \rightarrow s^1p^3$ (4.132 eV), and $s^2p^1 \rightarrow s^1p^2$ (5.310 eV), reproducing these energies with accuracy of better than 0.001 eV. The AO energies (-14.9712 eV and -7.7601 eV for $3s$ and $3p$ AOs, respectively) and Slater exponents (1.6344 and 1.4284 for $3s$ and $3p$ AOs, respectively) for neutral silicon atom were from Ref. 26. Note that other transitions, such as $s^2p^2(^3P_0) \rightarrow s^1p^3(^3D_1)$ etc., allow one to account for a multiplicity of electronic states in NTB, which will be the subject of future work.

The repulsive and ion-ion terms together include four parameters (two parameters for each of s and p -type AOs). The NTB matrix elements include 16 parameters—4 parameters for each type ($ss, sp, pp-\sigma, pp-\pi$) of matrix elements. A total of 20 parameters were fitted to the following data on small silicon clusters, Si_n , with $2 \leq n \leq 7$: (i) experimental³³ bond distance, binding energy, vibrational frequency, adiabatic electronic affinity³⁴ (EA), and ionization potential³⁵ (IP) of Si_2 , as well as bond distances in the cation Si_2^+ and anion Si_2^- computed at the MP2(full)/6-311G(3df,2p) level of theory: 2.258 Å and 2.118 Å, respectively; (ii) experimental³⁶ cohesive energies of Si_n with $3 \leq n \leq 7$, excepting Si_5 , for which the G2 theory result³⁷ was used; (iii) geometry of Si_n with $3 \leq n \leq 7$ obtained at the MP2/6-31G* level of theory³⁸ and given by two geometric parameters in each case: by two equal bond distances and angle between them for Si_3 , by side length and short diagonal of rhombus for Si_4 , by distance between two apex atoms and side of base polygons of trigonal (D_{3h}), tetragonal (D_{4h}), and pentagonal (D_{5h}) bipyramids for Si_5 , Si_6 , and Si_7 (Fig. 1), respectively. In addition, to maintain the correct ground state symmetry for neutral Si_2 ,³⁸ we forced the highest occupied level to be π -type and half filled. Table I presents values of our NTB parameters obtained using least-squares fitting.

Tables II and III illustrate the accuracy of the parametrization of the above properties of small silicon clusters with $2 \leq n \leq 7$ and of the prediction of IP and EA for $3 \leq n \leq 7$. Along with the rhombus geometry (D_{2h}) for Si_4 , trigonal

TABLE I. Fitted values of NTB parameters for silicon clusters (given with more precision than needed to avoid truncation errors).

Repulsive and ion-ion energies	a_s	α_s	a_p	α_p		
	4.718871	2.224932	17.115649	2.289726		
NTB matrix elements	b	$\beta/2$	γ (Bohr ⁻¹)	d (Bohr)		
H_{ss}	1.346041	0.708266	4.021170	5.746866		
H_{sp}	1.148782	0.741648	2.621936	7.249720		
$H_{pp\sigma}$	0.526912	0.392825	2.621936	7.249720		
$H_{pp\pi}$	0.350851	0.303682	2.621936	7.249720		
Energy of atoms	Δe_1	Δe_2	Δe_3	Δe_4	Δe_5	Δe_6
	0.091419	0.064977	-0.011790	0.042711	0.034672	-0.032179

(D_{3h}), tetragonal (D_{4h}), and pentagonal (D_{5h}) bipyramids have been found to be the lowest energy isomers (Fig. 1) for Si_5 , Si_6 , and Si_7 , respectively, in agreement with experiment and first-principles calculations. For Si_4 , the tetrahedral geometry, with T_d point group and four equal bond distances of 2.395 Å, was predicted to be 0.606 eV higher in energy than the rhombus geometry. The results of the NTB method (NTBM) for cohesive energies, IP and EA, are comparable in accuracy to the results of G2 theory,³⁷ diffusion Monte Carlo (DMC),³⁶ and density functional theory (DFT) with the generalized gradient approximation (GGA),³⁵ almost exactly coinciding with experimental data for electronic affinities (except Si_7)³⁴ and cohesive energies.³⁶ Note that our cohesive energies are larger than experimental ones by approximately the per atom zero-point energies calculated at MP2/6-31G(*d*) level.^{39,40}

The calculated bond distances deserve particular attention. *Ab initio* and conventional tight-binding calculations are in reasonably agreement for the shortest bond distances. However, they deviate noticeably in predicting larger bond distances. Conventional TB methods, including DFTB (Ref. 15) and TB,¹² which account for the nonorthogonality of AO, have a clear tendency to overestimate the shortest bond distances as well. The NTBM results, being in excellent agreement with *ab initio* results, overall tend to slightly underestimate (by 0.01–0.04 Å) bond lengths. The largest deviation, however, is observed for Si_3 ; the obtained bond distance and angle for Si_3 are 2.256 Å and 64.9°, respectively, compared to *ab initio* results at the QCISD(T)/6-31G* level of theory:³⁸ 2.191 Å and 79.6°, respectively. There is perhaps another local minimum in the multidimensional space of the NTBM parameters where this deficiency is absent (or can be removed by decreasing the accuracy of other results to some extent). However, we have not yet located such a parameter combination and overall we are satisfied with the results obtained using the present set of parameters.

The fitted NTB matrix elements and, consequently, Si-Si potential (Figs. 2 and 3) appeared to be short range, falling rapidly to zero for interatomic distances larger than that corresponding to the second-neighbor distance in bulk silicon. Therefore, a 64-atom supercell model of bulk silicon is quite reasonable for use with this NTB parametrization.

We calculated the cohesive energy, lattice constant, and band gap of Si using this model and one, $k=0$, point of the reciprocal lattice, to check transferability of our NTB parameters for the system with an infinite number of atoms. The predicted results are given in Table IV with a comparison with those of conventional TB (Refs. 11 and 19) and experiment. As seen from table, our results are in reasonably good agreement with experimental data, but for the lattice constant we obtained slightly worse results than those of conventional TB.^{11,19} This is partially because, unlike conventional TB methods, the present method did not include any bulk properties in the parametrization. This also reflects the small underestimation of bond lengths shown by the present NTB parametrization, which is reflected also in the bulk lattice parameter, and consequently, in the other two parameters. The cohesive energy and band gap calculated at the experimental lattice parameter are given also in Table IV, which demonstrates the possibility of achieving excellent agreement with all three parameters of bulk silicon using the NTB method.

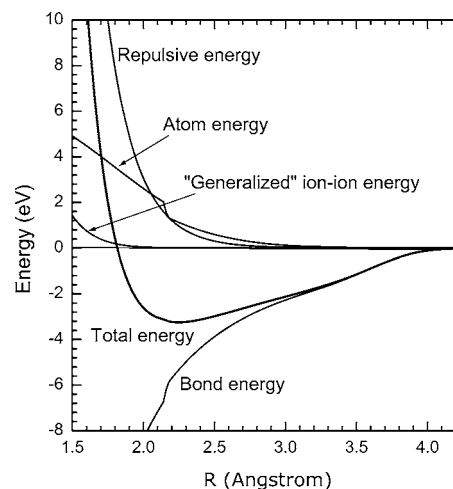


FIG. 2. Pair potential for Si and its NTB components. The sharp change in atom and bond energies at an interatomic distance around 2.15 Å is due to the alteration of order of π and σ MOs.

TABLE II. Cohesive and spectroscopic energies of small silicon clusters.

Method and reference No.	Si ₂	Si ₃	Si ₄	Si ₅	Si ₆	Si ₇
Cohesive energy per atom (eV)						
MP4/6-31G* (Ref. 38)	1.30	2.11	2.64	2.75	3.00	3.17
MP2/6-31G(<i>d</i>) (Ref. 39)	1.29	2.15	2.74		3.18	3.31
CCSD(T)/6-31G(<i>d</i>) (Ref. 40)	1.32	2.11	2.61		2.93	3.05
G2 theory (Ref. 37)	1.60	2.47	2.99	3.23	3.45 ^d	
LDA (Ref. 35)	1.97	2.93	3.51	3.79	4.00	4.15
GGA (Ref. 35)	1.76	2.54	3.04	3.27	3.44	3.56
DMC (Ref. 36)	1.58	2.37	2.86		3.26	3.43
DFTB (Ref. 18)	1.936	2.983	3.488	3.766	3.925	4.063
NTB (this work)	1.62	2.51	3.04	3.22	3.45	3.62
Nonorthogonal TB (Ref. 12)	1.65	2.66	3.33	3.43	3.63	3.75
TB (Ref. 19)	1.70	2.40	3.01	3.22		
TB (Ref. 11)	1.60	2.51	3.21	3.16		
Experiment (Ref. 36)	1.61	2.45	3.01		3.42	3.60
Adiabatic electronic affinity (eV)						
MRSDCI/(4 <i>s</i> 3 <i>p</i> 1 <i>d</i>) ^d				2.21	1.92	
G2 theory (Ref. 37)	2.25	2.24	2.06	2.36		
NTB, this work	2.18	2.35	2.12	2.62	2.39	2.56
Experiment (Ref. 34)	2.18	2.29	2.13	2.59		1.85
Ionization potential (eV)						
CCSD(T)/6-31G(<i>d</i>) (Ref. 40)	/7.87	/7.88	/8.09	/8.02	/7.84	/7.86
LDA (Ref. 35)	7.94/7.94 ^a	8.18/8.27	7.87/8.17	8.25/8.32	7.85/7.99	8.11/8.14
GGA (Ref. 35)	7.86/7.87	8.11/8.20	7.74/8.06	8.12/8.18	7.76/7.89	8.02/8.04
NTB (this work)	7.94/7.95	7.88/7.93	8.02/8.13	8.66/8.73	8.20/8.28	8.07/8.11
TB (Ref. 44) ^b	/8.09	/8.11	/7.70	/8.07	/8.27	/7.73
TB (Ref. 45) ^b	/8.24	/8.49	/7.95	/8.53	/8.42	/8.08
Experiment (Ref. 46)	7.94	7.97–8.49 ^c	7.97–8.49	7.97–8.49	7.97–8.49	~7.9

^aTwo values separated by slash are adiabatic and vertical IP, respectively.

^bThese TB are not designed for total energy calculations; they use geometries from other calculations and estimate IP using Koopmans' theorem.

^cReference 35.

^dReference 43.

IV. APPLICATION OF NTB FOR MEDIUM-SIZE SILICON CLUSTERS

Medium-size silicon clusters Si_{*n*} in the range of 8 ≤ *n* ≤ 20 have been already studied in detail by first-principles calculations (Refs. 35–42 and references therein), and available experimental data on ionic mobility and spectroscopic energies^{41,42} of Si clusters indirectly support the geometries predicted by these calculations. Therefore, the results of these calculations can be used for checking transferability and reliability of NTB for larger silicon clusters. On the other hand, there are still a great variety of unexplored isomers of silicon clusters that may also be consistent with the experimental data, and the experiments themselves may also be subject to correction. An intriguing finding from the first-principles calculations is that the lowest energy geometries for *n* ≥ 11 differ greatly between clusters that differ in size by only one atom, although they are mostly based on the

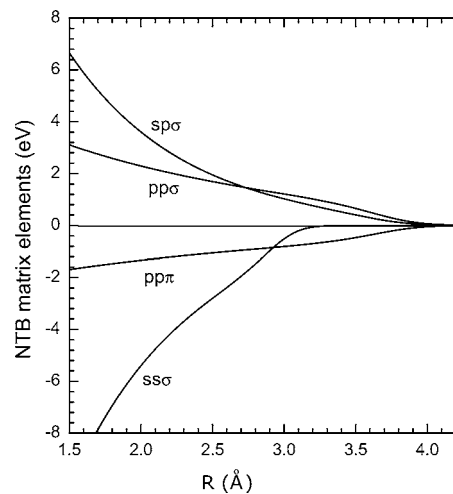


FIG. 3. NTB matrix elements for Si versus interatomic distance.

TABLE III. Characteristic bond distances (in Å) for small silicon clusters calculated by different methods. For Si_5 , Si_6 , and Si_7 , $R(1-2)$ is the distance between two apex atoms (Fig. 1), $R(1-3)$ is the distance between an apex atom and an atom on the base of the bipyramid, and $R(3-4)$ is the distance between neighboring atoms in the base of the bipyramid. For Si_4 the first and second values are the side and short diagonal of rhombus, respectively.

Method and reference No.	Characteristic bond distances	Si_3 (C_{2v})	Si_4 (D_{2h})	Si_5 (D_{3h})	Si_6 (D_{4h})	Si_7 (D_{5h})
MP2/6-31G* (Refs. 38 and 34)	$R(1-2)$	2.191 ^a	2.312	3.057	2.694	2.512
	$R(1-3)$	2.806 ^a	2.413	2.296	2.356	2.457
	$R(3-4)$			2.967	2.734	2.483
CASSCF/(3s3p1d) (Refs. 43)	$R(1-2)$			2.987	2.839	
	$R(1-3)$			2.346	2.403	
	$R(3-4)$			3.133	2.742	
NTBM (this work)	$R(1-2)$	2.256	2.299	3.047	2.683	2.502
	$R(1-3)$	2.420	2.410	2.298	2.348	2.423
	$R(3-4)$			2.980	2.724	2.439
Nonorthogonal TB (Refs. 12)	$R(1-2)$	2.239	2.336	3.253		2.799
	$R(1-3)$	2.800	2.516	2.356		2.527
	$R(3-4)$			2.845		2.474
TB (Refs. 19)	$R(1-2)$	2.28	2.34	2.94		
	$R(1-3)$	2.71	2.54	2.36		
	$R(3-4)$			3.20		
DFTB (Refs. 15)	$R(1-2)$	2.221	2.313	3.119		2.858
	$R(1-3)$	2.972	2.659	2.331		2.658
	$R(3-4)$			2.959		2.634

^aResults at the QCISD(T)/6-31G* level of theory.

tricapped trigonal prism unit.⁴² The actual growth pattern of clusters by sequential addition of single Si atoms or small Si clusters will not necessarily include only the lowest energy isomers, because high barriers or requirements for large atomic displacements may prevent rearrangement of each lowest energy isomer to the lowest-energy isomer of larger size, if these isomers are not structurally similar. Thus, from a slightly more practical point of view, regular (smooth) growth patterns of clusters are of interest.

Therefore, we decided to consider also a regular growth pattern initiated by Si_7 (Fig. 1), a pentagonal bipyramid. This growth pattern provides at least four bonds for each atom in the cluster, with the exception of Si_8 , Si_{14} , and Si_{20} , each of which has one three-coordinated atom. This pattern can be periodically repeated indefinitely, using a capped pentagon motif. One can always place a silicon atom above or below

the pentagon of Si_7 in such a way (Fig. 4, Si_8) that it can find three neighbors (two from the pentagon and one of the two capping atoms) at characteristic shortest interatomic distances (Table III). If one places a second atom in the same way above three atoms of Si_7 , such that it is also adjacent to the first silicon atom (Fig. 4, Si_9), the second and first atoms become four-coordinated atoms again at the same characteristic distances from each other. The same is true when the next two atoms are added. When one adds a fifth atom, it forms an additional bond with the first atom added, completing another pentagon (Fig. 4, Si_{12}). Capping this pentagon with a sixth atom, gives an icosahedral cluster (Fig. 4, Si_{13}), increasing the number of bonds by one for each atom in the pentagon. Such a construction of overcoordinated clusters can be continued infinitely in one direction (Fig. 4 depicts such clusters only up to Si_{19}). In this respect the Si_7 cluster is

TABLE IV. Bulk silicon properties calculated by different tight-binding models as compared to experiment.

Property	NTB (this work)	TB (Ref. 11)	TB (Ref. 19)	Experiment
Lattice constant (Å)	5.329	5.44	5.429	5.429 (Ref. 47)
Cohesive energy (eV/atom)	4.582 (4.56) ^a	4.66	4.62	4.63 (Ref. 48)
Band gap (eV)	0.87 (1.06) ^a	0.78	0.829	1.17 (Ref. 49)

^aValues in parentheses calculated at experimental lattice constant.

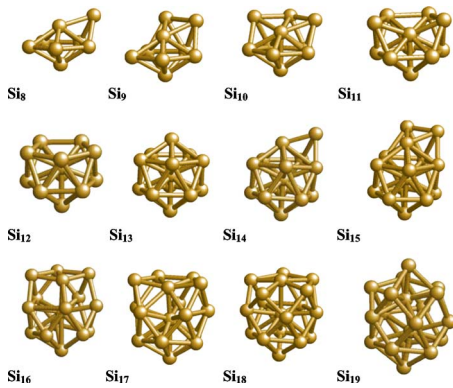


FIG. 4. (Color online) Optimized geometries of clusters from the regular growth pattern suggested in this work.

unique; the shape and aspect ratio of other small compact clusters cannot provide this possibility.

The geometry of the above clusters was optimized by molecular dynamics simulation with forces computed numerically using total energy calculations as described above. In addition, we considered the lowest energy isomers suggested in the literature for $n > 7$, reoptimizing the geometries of those clusters obtained at the MP2/6-31G(*d*) level of theory.^{39,40} The resulting geometries are shown in Figs. 4 and 5, respectively. In most cases, upon reoptimization using NTB, the MP2/6-31G(*d*) geometries preserved their original shape and topology. For Si₁₁ the tricapped tetragonal antiprism geometry was subjected to some distortion, while for Si₁₅ the tricapped trigonal prism unit was transformed completely into capped tetragonal antiprism (see lower part of Figure 5, Si₁₅). We had some convergence difficulties in the case of Si₁₉, but eventually this cluster stabilized with a more spherical shape than that predicted by *ab initio* calculations (Fig. 6).

Figure 7 depicts the cohesive energy per atom (EPA) for clusters from both growth patterns, calculated by the present NTB method, as compared to *ab initio* and DFTB calculations. Our calculations, which are in the best agreement with experiment (see also Table II) for small clusters ($n \leq 7$), reproduce quite well the MP2/6-31G(*d*) EPA,^{39,40} scaled by us as in Ref. 38 for larger clusters. Note that this scaling has a tendency to overestimate EPA of clusters with $n > 3$. Our

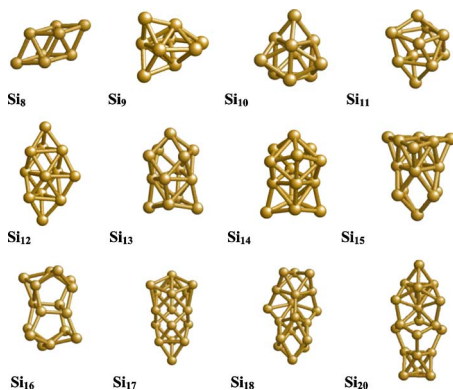


FIG. 5. (Color online) Reoptimized geometries of clusters from Refs. 39 and 40; for Si₁₉, see Fig. 6.

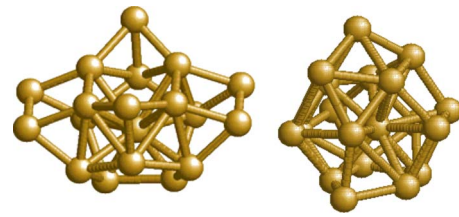


FIG. 6. (Color online) Geometry of Si₁₉ from Ref. 40 before (on the left) and after (on the right) reoptimization by NTB.

results for the MP2/6-31G(*d*) reoptimized geometries correct (curve 6') to some extent these scaling errors, being always lower than the scaled values. Note our results' smooth peculiarities of EPA in the range $6 < n < 12$, and DFTB does so as well (curve 4'). In fact, one can see this tendency in *ab initio* results with increasing levels of theory (compare curves 4 and 5, curves 2 and 3) for large clusters too.

The EPA for clusters from the regular growth pattern was larger than for clusters from Refs. 39 and 40, as shown in Fig. 7. Exceptions were Si₁₁ and Si₁₉. However, the latter more nearly belongs to the family of clusters from the regular growth pattern, due to its drastic shape transformation and change of bond topology (Fig. 6) upon reoptimization with NTB. Examination of the differences in total energies for the two growth patterns, as well as the NTB component terms (Fig. 8), helps to explain this. First of all, from Fig. 8 one can see clear anticorrelation between differences of bond energies and atom energies, as well as between their difference and the difference of repulsive energies. This has a simple explanation: an increase in coordination number (or number of bonds) and decrease in interatomic distances (chemical bonds) leads to increases in both repulsive energy and the energy of individual atoms, promoting them to excited states (charge transfer from *s*- to *p*-AO increases). Bond energy also increases with increasing coordination number and decreasing interatomic distances. As seen in Fig. 8, the component energy terms are consistently larger for

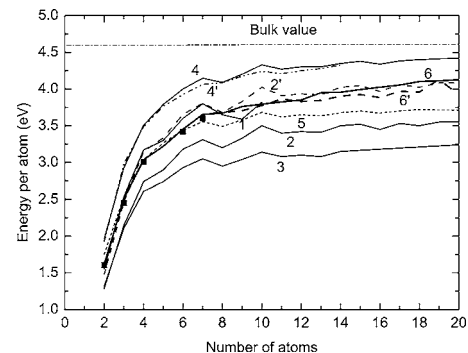


FIG. 7. Cohesive energy per atom for Si clusters calculated by different methods. 1—scaled MP4/6-31G* (Ref. 38); 2 and 2'—non-scaled and scaled (by us) MP2/6-31G(*d*) (Refs. 39 and 40); 3—CCSD(T)/6-31G(*d*) (Refs. 39 and 40); 4 and 4'—LDA (Ref. 35) and DFTB (Ref. 18), respectively; 5—GGA (Ref. 35); 6 and 6'—NTB for the regular growth pattern and for reoptimized geometries of MP2/6-31G(*d*) calculations (Refs. 39 and 40), respectively. The squares are experimental values (Ref. 36).

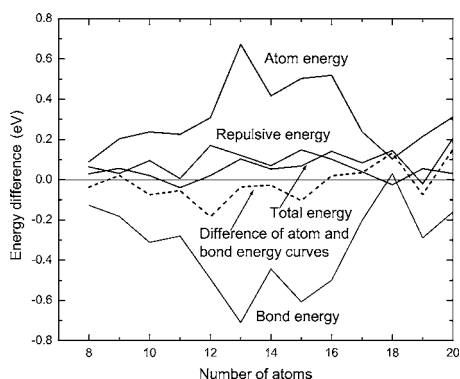


FIG. 8. Differences in total energy per atom and in the NTB component terms between clusters from the regular growth pattern and reoptimized clusters from Refs. 39 and 40. The values for the former are subtracted from the corresponding values for the latter. Results for the ion-ion term, which are negligible on the scale of this plot, are not shown.

clusters from Refs. 39 and 40 with the minor exceptions of one term each for Si_{18} and Si_{19} . However, the resulting total energy differences favor the clusters from the regular growth pattern. This seems to result from the existence of more short bonds in the clusters based on the *ab initio* calculations compared to clusters from the regular growth pattern. According to the NTB calculations, the existence of these shorter bonds results in a greater increase in the atom energies and repulsive energies than lowering of the bond energy, with the net result that the structures from the smooth growth pattern are predicted to be more stable. Bonds shorter than 2.30 Å are common for both the initial and reoptimized clusters from Ref. 40, while for clusters from the regular pattern such bonds are only found between internal atoms in clusters Si_{19} and Si_{20} . In addition, reoptimization of the cluster geometries from Ref. 40 using NTBM leads to decreases in bond distances of up to 0.12 Å for bonds with lengths of up to 2.60 Å (excluding Si_{19}). This is consistent with the general trend toward prediction of shorter bond lengths by NTB compared to MP2/6-31G(*d*). Whether this may stabilize clusters from the regular growth pattern compared to those from the pattern established by *ab initio* calculations is not clear. It is possible that shorter bond distances, predicted by NTB, may mimic *ab initio* calculations with larger basis sets, which are not yet available for clusters of this size. On the other hand, underprediction of bond lengths may simply reflect remaining deficiencies in the present parametrization of NTB.

Figure 9 compares the vertical IP calculated by NTB to results of *ab initio* calculations and experiment. As seen there, our results for both growth patterns are in reasonable agreement with the latter, reflecting the general tendency of IP to decrease with increasing cluster size, as well as some peaks of IP for large clusters. Though these peaks are absent in the regular growth pattern case, the remaining results for this pattern are in reasonable quantitative agreement with experiment. Overall, the IP for reoptimized clusters from Refs. 39 and 40, though mostly overestimated by NTB, seem to be in better agreement with experiment with respect to the qualitative peculiarities of IP changes with cluster size, compared to clusters from the regular growth pattern. Note that

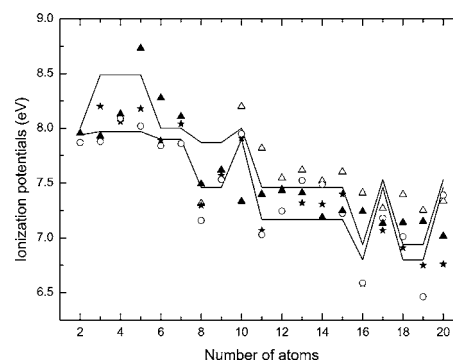


FIG. 9. Vertical IP of Si clusters calculated by different methods: stars—GGA (Ref. 35); circles—CCSD(T)/6-31G(*d*) (Refs. 39 and 40); filled and open triangles—NTB for regular growth pattern and for reoptimized clusters from Refs. 39 and 40, respectively. When both triangles coincide, only filled triangles are seen. Lines—experimental lower and upper limits for IP (Refs. 46 and 35).

overall underestimation of the vertical IP of silicon clusters is characteristic of *ab initio* calculations. All this, of course, indicates not only deficiencies of the current implementation of theories and possibly missed ground state geometries but, perhaps, the necessity for more precise experimental identification and characterization of silicon clusters.

Figure 10 presents vertical electron detachment energies (VDE), calculated by NTB and GGA,⁴² as compared to the experimental values.⁴² As seen there, our results for reoptimized clusters from Refs. 39 and 40 reproduce the experimental tendency of increase in VDE with increasing cluster size quite well. However, peculiarities for clusters with 8, 9, and 16 atoms are not reproduced. Overall, the NTB results overestimate the VDE for large clusters, though deviation of these results from the experiment is frequently of the same order as that of GGA results. The results for clusters from the regular growth pattern deviate substantially from experimental data, mostly underestimating the VDE for large clusters.

Thus, our results on IP and VDE as a whole seem to favor the growth pattern established by *ab initio* calculations as compared to the regular growth pattern. However, the opposite is true based on predictions of energy per atom. This may reflect remaining deficiencies of the present parametrization of NTB, the improvement of which will be the subject

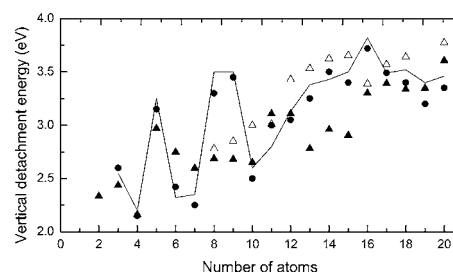


FIG. 10. Vertical electron detachment energy of Si clusters: circles—GGA (Ref. 42); filled and open triangles—NTB for regular growth pattern and for reoptimized clusters from Refs. 39 and 40, respectively; when both triangles coincide, only filled triangles are seen. Lines—the experimental values (Ref. 42). Experimental and GGA values reproduced from Fig. 3 in Ref. 42.

of future work. In practice, it is not only the electronic energy of clusters, considered here, that determines the observed cluster structures, but also thermal energy, entropy, and the kinetic accessibility of the different structures. The predicted energy differences between the two growth patterns are small, and therefore these other factors could be particularly important.

V. CONCLUSIONS

In summary, the principal differences between conventional tight-binding methods and the nonconventional tight-binding method¹⁴ have been highlighted and the latter has been developed and parametrized for simulation of the structures, cohesive energies, ionization potentials, and electron affinities of silicon clusters. All of the above properties have been described with accuracy comparable to state-of-the-art *ab initio* methods using a single TB model. Conventional TB models have not been able to do this mainly because of (i) underestimation of individual properties of chemical elements, (ii) underestimation of the role of self-consistent calculations of intra- and interatomic charge redistributions, which naturally account for different atomic environments without introduction of *ad hoc* parameters, and (iii) using an inconvenient total energy functional (1) with a repulsive term of complex and rather long-range character that is responsible, in particular, for systematic and mostly strong overestimation of bond distances by conventional TB.

NTB is based on a semiempirical total energy functional with four easily interpretable energy terms that are initially defined in terms of individual characteristics of chemical elements, and, consequently, are available for all elements of the Periodic Table. Thus, NTB is in fact a TB method with

broad possibilities for systematic improvement in the accuracy of the method based on understanding of the chemistry and physics of each element. Significant improvement of NTB likely can be achieved by further increasing the accuracy of, first of all, the atom energy term with accounting for multiplicity of atomic electronic states, because the majority of electronic correlation effects are inside the atomic sphere. This enables one to treat more adequately atomic clusters and remove the main deficiencies of the basic NTB parametrization. It is easy to observe the overall decrease of total electron spin on each atom in the sequence from silicon atom (2) to Si₂ (1) and further with increase of cluster size (average spin value is always below 1 and approaches 0). This increases the atom energy term toward positive values, lowering the cohesive energy of clusters, calculated in this work, toward accurate GGA energies.³⁵ This obviously improves the description of IP and EA as well, allowing one to distinguish neutral and charged states with respect to their spin states. This may also improve the results for the geometry of the Si₃ cluster, for which the lowest triplet state lies just 0.1–0.2 eV above the singlet ground state.³⁸ Work in this direction is in progress.

ACKNOWLEDGMENTS

The research described in this publication was made possible in part by financial support from the U.S. Civilian Research & Development foundation for Independent States of the Former Soviet Union (CRDF) and Grant No. Φ-2.1.18 of the Center for Science and Technology of the Ministerial Cabinet of the Republic of Uzbekistan. The authors are grateful to L.A. Curtiss for helpful discussion and X.C. Zeng for providing MP2/6-31G(*d*) geometries for Si_{*n*} (*n* ≥ 12).

*Electronic address: khakimov@inp.uz

- ¹J. C. Slater and C. F. Koster, Phys. Rev. **94**, 1498 (1954); A. V. Podolskiy and P. Vogl, Phys. Rev. B **69**, 233101 (2004).
- ²W. A. Harrison, *Electronic Structure and the Properties of Solids* (Freeman, San Francisco, 1980).
- ³D. J. Chadi, Phys. Rev. B **19**, 2074 (1979).
- ⁴D. Tomanek and M. A. Schluter, Phys. Rev. Lett. **56**, 1055 (1986).
- ⁵W. M. Foulkes and R. Haydock, Phys. Rev. B **39**, 12520 (1989).
- ⁶L. Goodwin, A. J. Skinner, and D. G. Pettifor, Europhys. Lett. **9**, 701 (1989).
- ⁷S. Sawada, Vacuum **41**, 612 (1990).
- ⁸K. Laasonen and R. Nieminen, J. Phys.: Condens. Matter **2**, 1509 (1990).
- ⁹A. P. Sutton, *Electronic Structure of Materials* (Oxford University Press, Oxford, 1993).
- ¹⁰J. L. Mercer, Jr. and M. Y. Chou, Phys. Rev. B **49**, 8506 (1994).
- ¹¹I. Kwon, R. Biswas, C. Z. Wang, K. M. Ho, and C. M. Soukoulis, Phys. Rev. B **49**, 7242 (1994).
- ¹²P. Ordejon, D. Lebedenko, and M. Menon, Phys. Rev. B **50**, 5645 (1994).
- ¹³K. Stokbro, N. Chetty, K. W. Jacobsen, and J. K. Nørskov, Phys.

Rev. B **50**, 10727 (1994).

- ¹⁴Z. M. Khakimov, Comput. Mater. Sci. **3**, 95 (1994).
- ¹⁵Th. Frauenheim, F. Weich, T. Kohler, S. Uhlmann, D. Porezag, and G. Seifert, Phys. Rev. B **52**, 11492 (1995).
- ¹⁶A. P. Horsfield, A. M. Bratkovsky, M. Fearn, D. G. Pettifor, and M. Aoki, Phys. Rev. B **53**, 12694 (1996).
- ¹⁷K. Colombo, in *Annual Reviews of Computational Physics*, edited by D. Stauffer (World Scientific, Singapore, 1996), Vol. IV.
- ¹⁸A. Sieck, D. Porezag, Th. Frauenheim, M. R. Pederson, and K. Jackson, Phys. Rev. A **56**, 4890 (1997).
- ¹⁹T. J. Lenosky, J. D. Kress, I. Kwon, A. F. Voter, B. Edwards, D. F. Richards, S. Yang, and J. B. Adams, Phys. Rev. B **55**, 1528 (1997).
- ²⁰L. J. Lewis and N. Mousseau, Comput. Mater. Sci. **12**, 210 (1998); G. Galli, *ibid.* **12**, 242 (1998).
- ²¹A. N. Andriotis and M. Menon, Phys. Rev. B **59**, 15942 (1999).
- ²²P. D. Goodwin, A. K. Roberts, D. Yu, K. Dean, and P. Clancy, Comput. Mater. Sci. **21**, 135 (2001).
- ²³K. A. Jackson, M. Horoi, I. Chaudhuri, T. Frauenheim, and A. A. Shvartsburg, Phys. Rev. Lett. **93**, 013401 (2004).
- ²⁴Th. Frauenheim, G. Seifert, M. Elstner, Z. Hajnal, G. Jungnickel, D. Porezag, S. Suhai, and R. Scholz, Phys. Status Solidi B **217**,

- 41 (2000); M. Elstner, Th. Frauenheim, E. Kaxiras, G. Seifert, and S. Suhai, *ibid.* **217**, 357 (2000); F. Della Sala, J. Widany, and Th. Frauenheim, *ibid.* **217**, 565 (2000).
- ²⁵Z. M. Khakimov, A. P. Mukhtarov, and A. A. Levin, *Semiconductors* **28**, 344 (1994); A. P. Mukhtarov, N. T. Sulaymonov, D. S. Pulatova, and Z. M. Khakimov, *ibid.* **28**, 587 (1994); Z. M. Khakimov, A. P. Mukhtarov, F. T. Umarova, and A. A. Levin, *ibid.* **28**, 959 (1994); Z. M. Khakimov, in *MRS Symposia Proceeding No. 527* (Materials Research Society, Pittsburgh, 1998), p. 369.
- ²⁶E. Clementi and D. I. Raimodi, *J. Chem. Phys.* **38**, 2686 (1963); **47**, 1300 (1967).
- ²⁷M. C. Zerner and M. Hehenberger, *Chem. Phys. Lett.* **62**, 550 (1979).
- ²⁸A. G. Maslov, *Zh. Strukt. Khim.* **20**, 761 (1979) [in Russian].
- ²⁹M. P. Allen and D. J. Tildesley, *Computer Simulation of Liquids* (Clarendon Press, Oxford, 1987).
- ³⁰Z. M. Khakimov, *Comput. Phys. Commun.* **147**, 731 (2002); Z. M. Khakimov, F. T. Umarova, N. T. Sulaymonov, A. E. Kiv, and A. A. Levin, *Int. J. Quantum Chem.* **93**, 351 (2003).
- ³¹E. Rougier, A. Munjiza, and N. W. M. John, *Int. J. Numer. Methods Eng.* **61**, 856 (2004).
- ³²A. A. Radtsig, B. M. Smirnov, *Parameters of Atoms and Atomic Ions: Handbook* (Moscow, Energoatomizdat, 1986) [in Russian].
- ³³*Molecular Constants of Inorganic Compounds: Handbook*, edited by K. S. Krasnov (Moscow, Khimiya, 1979) [in Russian].
- ³⁴C. Xu, T. R. Taylor, G. R. Burton, and D. M. Neumark, *J. Chem. Phys.* **108**, 1395 (1998).
- ³⁵B. Liu, Z. Y. Lu, B. Pan, C. Z. Wang, K. M. Ho, A. A. Shvartsburg, and M. F. Jarrold, *J. Chem. Phys.* **109**, 9401 (1998).
- ³⁶J. C. Grossman and L. Mitas, *Phys. Rev. Lett.* **74**, 1323 (1995).
- ³⁷L. A. Curtiss, P. W. Deutsch, and K. Raghavachari, *J. Chem. Phys.* **96**, 6868 (1992).
- ³⁸K. Raghavachari and C. M. Rohlfing, *J. Chem. Phys.* **89**, 2219 (1988); **96**, 2114 (1992).
- ³⁹X. L. Zhu and X. C. Zeng, *J. Chem. Phys.* **118**, 3558 (2003).
- ⁴⁰X. L. Zhu, X. C. Zeng, Y. A. Lei, and B. Pan, *J. Chem. Phys.* **120**, 8985 (2004).
- ⁴¹K. M. Ho, A. A. Shvartsburg, B. Pan, Z. Y. Lu, C. Z. Wang, J. G. Wacker, J. L. Fye, and M. F. Jarrold, *Nature (London)* **392**, 582 (1998).
- ⁴²J. Muller, B. Liu, A. A. Shvartsburg, S. Oqut, J. R. Chelikowsky, K. W. Michael Siu, K. M. Ho, and G. Gantefor, *Phys. Rev. Lett.* **85**, 1666 (2000).
- ⁴³C. Zhao and K. Balasubramanian, *J. Chem. Phys.* **116**, 3690 (2002).
- ⁴⁴J. Zhao, X. Chen, Q. Sun, F. Liu, and G. Wang, *Phys. Lett. A* **198**, 243 (1995).
- ⁴⁵C. Jo and K. Lee, *J. Korean Phys. Soc.* **32**, 182 (1998).
- ⁴⁶K. Fuke, K. Tsukamoto, F. Misaizu, and M. Sanekata, *J. Chem. Phys.* **99**, 7807 (1993).
- ⁴⁷J. Donohue, *The Structure of the Elements* (Wiley, New York, 1974).
- ⁴⁸C. E. Moore, *Atomic Energy Levels*, Natl. Bur. Stand. (U. S.) Circ. No 467 (U.S. GPO, Washington, D.C., 1949), Vol. I.
- ⁴⁹W. Bludau, A. Onton, and W. Heinke, *J. Appl. Phys.* **45**, 1846 (1974); K. L. Shalee and R. E. Nahony, *Phys. Rev. Lett.* **24**, 942 (1970).